Infrared Spectra of the OH^+ and H_2O^+ Cations Solvated in Solid Argon

Han Zhou, Rongjing Yang, Xi Jin, and Mingfei Zhou*

Department of Chemistry & Laser Chemistry Institute, Shanghai Key Laboratory of Molecular Catalysts and Innovative Materials, Fudan University, Shanghai 200433, People's Republic of China

Received: March 7, 2005; In Final Form: May 20, 2005

Infrared spectra of various OH^+ and H_2O^+ isotopomers solvated in solid argon are presented. The OH^+ and H_2O^+ cations were produced by co-deposition of H_2O/Ar mixture with high-frequency discharged Ar at 4 K. Detailed isotopic substitution studies confirm the assignments of absorptions at 3054.9 and 3040.0 cm^{-1} to the antisymmetric and symmetric H−O−H stretching vibrations of H_2O^+ and 2979.6 cm^{-1} to the O−H stretching vibration of OH^+. The frequencies of H_2O^+ solvated in solid argon are red-shifted, whereas the frequency of OH^+ is blue-shifted with respect to the gas-phase fundamentals. On the basis of previous gas-phase studies and quantum chemical calculations, the OH^+ and H_2O^+ cations solvated in solid argon may be regarded as the OH^+-Ar_5 and $H_2O^+-Ar_4$ complexes isolated in the argon matrix.

Introduction

The hydroxyl and water cations are important transient intermediates in many chemical processes, such as the chemistry of earth's atmosphere, interstellar space, and hydrogen- and oxygen-containing plasmas. The ground states as well as some excited states of the OH^+ and H_2O^+ cations have been extensively studied in the gas phase by various spectroscopic methods[1−16] and by quantum chemical calculations.[17−25] Recently, the infrared spectra of the OH^+−and H_2O^+−rare gas atom open-shell ionic complexes have been obtained by photofragmentation spectroscopy in a tandem mass spectrometer.[26−29] Rotationally resolved infrared spectra revealed that the OH^+−He and OH^+−Ne complexes possess linear proton-bound equilibrium structures,[26] in agreement with quantum chemical simulations.[30−32] Infrared spectra of H_2O^+-Ne[27] and $H_2O^+-Ar_n$ ($n = 1-14$)[28,29] in the vicinity of the O−H stretching vibrations of the water cation indicated that the H_2O^+-Ar and H_2O^+-Ne complexes have a planar proton-bound equilibrium geometry; the most stable $H_2O^+-Ar_2$ geometry has two equivalent intermolecular H-bonds. The $H_2O^+-Ar_2$ core could further be solvated by two argon atoms attached to the opposite sites of the 2p orbital of oxygen ($n = 3, 4$) and subsequently by less strongly bound Ar atoms to form an Ar solvation shell. The O−H stretching frequencies of OH^+ and H_2O^+ are red-shifted when they are complexed by noble gas atoms.[28] Ab initio and density functional calculations on $H_2O^+-Ar_n$ ($n = 0-4$) predicted that the most stable structures of $H_2O^+-Ar_n$ ($n = 1-4$) have C_s symmetry ($n = 1, 3$) and C_{2v} symmetry ($n = 2, 4$).[33]

The OH^+ and H_2O^+ cations embedded in solid rare gas matrixes can be regarded as OH^+-Ng_n and $H_2O^+-Ng_n$ with $n = \infty$ (Ng denotes rare gas atoms). The band shifts of matrix-isolated OH^+ and H_2O^+ with respect to the gas-phase values provide useful information in determining how many rare gas atoms are necessary to close the first solvation shell and to make the band shift converged. The H_2O^+ cation has been isolated in solid neon.[34] The two stretching frequencies of H_2O^+ isolated in solid neon appear approximately 1% below the gas-phase values. No argon matrix isolation studies on H_2O^+ and OH^+ have been reported. In this paper, we report an infrared absorption spectroscopic study of the H_2O^+ and OH^+ cations solvated in solid argon.

Experimental and Computational Methods

The H_2O^+ and OH^+ cations in solid argon were prepared by high-frequency discharge. The experimental setup for high-frequency discharge and matrix isolation FTIR spectroscopic investigation has been described in detail previously.[35,36] Briefly, two gas streams containing pure argon and H_2O/Ar mixture were co-deposited with an approximately equal amount onto a CsI window cooled normally to 4 K by means of a closed-cycle helium refrigerator. The pure argon gas stream was subjected to discharge with a high-frequency generator (Tesla coil). The tip of the Tesla coil was connected to a copper cap on one end of a quartz tube extending into the vacuum chamber. The other end of the quartz tube was connected to a copper tube with ground potential. Discharge takes place between the cap and the copper tube. The matrix gas deposition rate was typically of 2−4 mmol per hour. In general, matrix samples were deposited for 1−2 h.

The H_2O/Ar mixtures were prepared in a stainless steel vacuum line using standard manometric technique. Distilled water and isotopic D_2O and $H_2{}^{18}O$ (Cambridge Isotopic Laboratories) and selected mixtures were used in different experiments. H_2O was cooled to 77 K using liquid N_2 and was evacuated to remove volatile impurities. D_2O and $H_2{}^{18}O$ were used without further purification. Isotopic exchange with water adsorbed on the walls of the vacuum line occurred readily. In the experiments with the D_2O sample, HDO and H_2O absorptions were also presented.

The infrared absorption spectra of the resulting sample were recorded on a Bruker Equinox 55 spectrometer at a resolution of 0.5 cm^{-1} between 4000 and 400 cm^{-1} using a DTGS detector. After the infrared spectrum of the initial deposit had been recorded, the sample was subjected to broad-band irradiation using a high-pressure mercury arc lamp with glass filters, and

* Author to whom correspondence should be addressed. E-mail: mfzhou@fudan.edu.cn.

10.1021/jp0511808 CCC: $30.25
Published on Web 06/21/2005

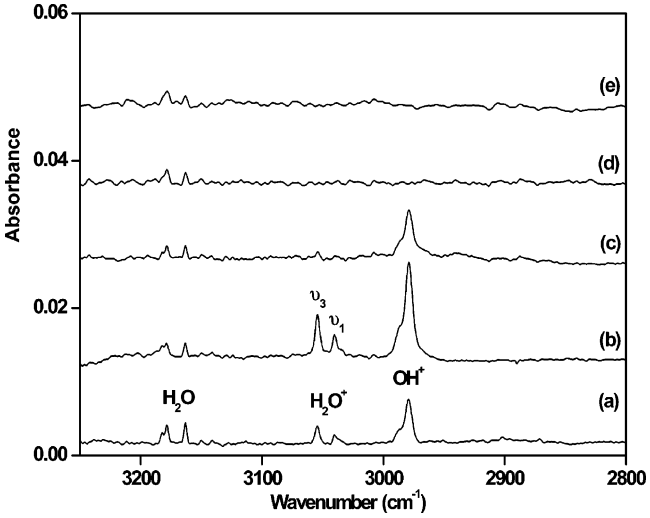

Figure 1. Infrared spectra in the 3250−2800 cm^{-1} region from co-deposition of H_2O/Ar with discharged Ar at 4 K. (a) 0.2% H_2O, 1 h of sample deposition, (b) 0.2% H_2O + 0.02% CCl_4, 1 h of sample deposition, (c) 20 min irradiation (λ > 400 nm) of sample b, (d) 20 min irradiation (λ > 290 nm) of sample c, and (e) 25 K annealing of sample d.

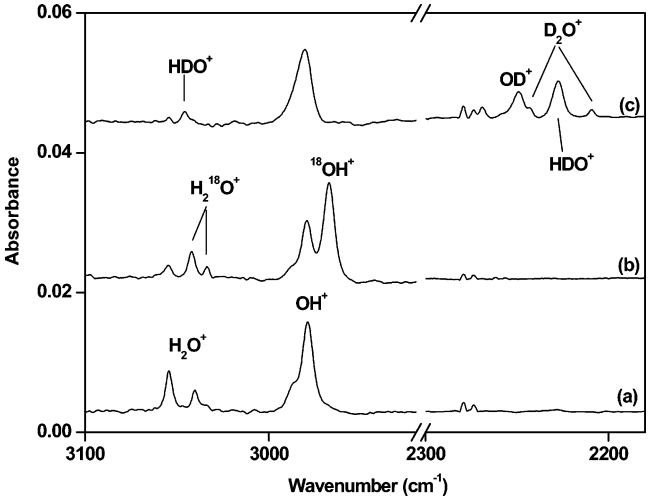

Figure 2. Infrared spectra in the 3100−2920 and 2300−2180 cm^{-1} regions from co-deposition of H_2O/Ar with discharged Ar at 4 K. (a) 0.15% H_2O/0.015% CCl_4/Ar, (b) 0.1% $H_2{}^{16}O$/0.2% $H_2{}^{18}O$/0.02% CCl_4/Ar, and (c) 0.1% H_2O/0.2% HDO/0.2% D_2O/0.02% CCl_4/Ar.

TABLE 1: Infrared Absorptions (cm^{-1}) of Different OH^+ and H_2O^+ Isotopomers in Solid Argon

ν_1	ν_3	
3040.0	3054.9	$H_2{}^{16}O^+$
3033.7	3042.5	$H_2{}^{18}O^+$
3046.1	2227.4	$HD^{16}O^+$
2209.4	2243.1	$D_2{}^{16}O^+$
2979.6		$^{16}OH^+$
2967.2		$^{18}OH^+$
2249.1		$^{16}OD^+$

selected samples were annealed to different temperatures and more spectra were taken.

Quantum chemical calculations were performed on the OH^+−Ar_n and H_2O^+−Ar_n complexes using the Gaussian 03 program.[37] The Becke's three-parameter hybrid functional with the Lee−Yang−Parr correlation corrections (B3LYP) as well as the second-order Moller−Plesset perturbation theory (MP2) were used.[38,39] The 6-31++G(d, p) basis set was used for MP2 calculations, while the 6-311++G(3df, 3pd) basis set was used for B3LYP calculations.[40] The geometries were fully optimized; the harmonic vibrational frequencies were calculated with analytic second derivatives.

Results and Discussion

Infrared Spectra. A series of experiments have been done using various H_2O concentrations (ranging from 0.05% to 0.5% in argon) and various discharge powers. In addition to the strong H_2O and $(H_2O)_2$ absorptions, condensation of H_2O/Ar with high-frequency-discharged Ar at 4 K produced new absorptions at 3547.9, 3451.6, 3054.9, 3040.0, and 2979.6 cm^{-1}. The 3547.9 cm^{-1} band was previously assigned to the OH radical.[41] The 3451.6 cm^{-1} band is due to the H_2O−OH complex.[42] The 3054.9, 3040.0, and 2979.6 cm^{-1} bands have never been reported in previous discharge experiments. The intensities of the product absorptions depended strongly on the power levels of discharge. The OH and H_2O−OH absorptions were strong at high power of discharge, whereas the 3054.9, 3040.0, and 2979.6 cm^{-1} absorptions were favored with relatively lower power of discharge. Weak HOO absorptions at 3412.1, 1388.3, and 1100.7 cm^{-1}[43] were also observed at high power of discharge. The spectra in the 3240−2800 cm^{-1} frequency region are shown in Figure 1. Trace a shows the spectrum taken after 1 h of co-deposition of 0.2% H_2O in argon with discharged Ar at 4 K. Traces b−e show the spectra from another experiment with the same experimental conditions as trace a but with 0.02% CCl_4 doped in the reagent gas. The OH and H_2O−OH neutral absorptions are about the same with and without CCl_4 doping, but the intensities of the 3054.9, 3040.0, and 2979.6 cm^{-1} absorptions in the CCl_4 doping experiment (trace b) are about twice as strong as those without CCl_4 doping (trace a). Twenty minutes of broad-band irradiation with a 400-nm-long wavelength pass filter (400 < λ < 580 nm) destroyed the 3054.9 and 3040.0 cm^{-1} bands and halved the 2979.6 cm^{-1} band (trace c). The 2979.6 cm^{-1} band disappeared on another 20 min of broad-band irradiation with a 290-nm-long wavelength pass filter (290 < λ < 580 nm) (trace d). These absorptions cannot be recovered on sample annealing to 25 K (trace e) after broad-band irradiations.

Similar experiments were also done using isotopic labeled $H_2{}^{18}O$, D_2O, and $H_2{}^{16}O$ + $H_2{}^{18}O$, H_2O + HDO + D_2O mixtures for product identification on the basis of isotopic shifts and splittings. The infrared spectra in the 3100−2920 and 2300−2180 cm^{-1} regions from co-deposition of various isotopic samples with discharged Ar at 4 K are illustrated in Figure 2. The band positions of the new product absorptions with different isotopic samples are listed in Table 1.

H_2O^+. The new absorptions at 3054.9, 3040.0, and 2979.6 cm^{-1} are photosensitive, which suggests that these absorptions are due to charged species. The charged species identification can be verified by CCl_4 doping. The role of CCl_4 as an electron trap in laser-ablation experiments and in discharge experiments has been discussed.[44,45] The CCl_4 molecule has high electron capture cross section. During sample condensation, the added CCl_4 molecules capture most of the electrons produced by discharge, thus reducing the yield of other anions and facilitating the survival of more cations. As demonstrated in Figure 1, the intensities of the 3054.9, 3040.0, and 2979.6 cm^{-1} absorptions increased relative to the neutral OH and H_2O−OH absorptions, which indicates that the new product absorptions are due to positively charged species.

The 3054.9 and 3040.0 cm^{-1} bands can be grouped together because of their consistent behavior upon irradiation and annealing, indicating that they are due to different vibrational

modes of the same species. These two bands shifted to 3042.5 and 3033.7 cm^{-1} with $H_2{}^{18}O$/Ar and to 2243.1 and 2209.4 cm^{-1} with the D_2O/Ar sample, which gave the isotopic $^{16}O/^{18}O$ ratios of 1.0041 and 1.0021 and the H/D ratios of 1.3619 and 1.3759, respectively. These ratios are characteristic of HOH stretching vibrations. The 3054.9 cm^{-1} band exhibits a slightly larger $^{16}O/^{18}O$ ratio and a smaller H/D ratio than the 3040.0 cm^{-1} band. The 3054.9 cm^{-1} band is appropriate for an antisymmetric, while the 3040.0 cm^{-1} band is appropriate for a symmetric HOH stretching mode. The spectrum with a mixed $H_2{}^{16}O + H_2{}^{18}O$ sample (Figure 2, trace b) clearly shows that only one O atom is involved in the vibrational modes. In the spectrum with a mixed $H_2O + HDO + D_2O$ sample (Figure 2, trace d), two intermediate absorptions at 3046.1 and 2227.4 cm^{-1} were observed, which indicates that two equivalent H atoms are involved. The above-mentioned experimental observations pointed to the assignment of the 3054.9 and 3040.0 cm^{-1} bands to the antisymmetric (ν_3) and symmetric (ν_1) HOH stretching vibrations of the H_2O^+ cation. The 3046.1 and 2227.4 cm^{-1} absorptions in the mixed experiments are due to the H−O and D−O stretching modes of the HDO^+ cation. The bending mode of H_2O^+ is expected to be much weaker than the two stretching modes and was not observed in the present experiments.

The spectra and electronic structures of H_2O^+ have been the subject of considerable experimental and theoretical studies. The band centers of the antisymmetric and symmetric HOH stretching vibrations of the ground-state H_2O^+ cation were determined to be 3259.0 and 3212.6 cm^{-1} in the gas phase.[12] These two modes were observed at 3219.5 and 3182.7 cm^{-1} in solid neon matrix,[34] which deviate by 1.2% and 0.9% from the gas-phase band centers. These modes of the H_2O^+ cation in solid argon were observed at 3054.9 and 3040.0 cm^{-1}, which were red-shifted by 204.1 cm^{-1} (6.3%) and 172.6 cm^{-1} (5.4%) from the gas-phase band centers, respectively. These deviations are much larger than the matrix shifts observed for the ground-state fundamentals of most transient species isolated in solid argon.[46] Such large matrix shifts suggest that strong interactions between H_2O^+ and rare gas atoms should be considered.

Complexes of H_2O^+ with Ar have been identified in the previous mass spectrometric studies.[47,48] More recently, the infrared photodissociation spectra of $H_2O^+-Ar_n$ complexes with $n = 1-14$ in the gas phase have been recorded.[28] The H_2O^+-Ar and $H_2O^+-Ar_2$ complexes were determined to be proton-bound. The ν_1 and ν_3 modes were observed at 2630 and 3284 cm^{-1} for H_2O^+-Ar and at 2821 and 2875 cm^{-1} for $H_2O^+-Ar_2$. The $H_2O^+-Ar_3$ and $H_2O^+-Ar_4$ geometries were interpreted as one or two argon atoms attached to opposite sites of the O 2p orbital of the C_{2v} symmetric $H_2O^+-Ar_2$, that is, structures with C_s and C_{2v} symmetry for $H_2O^+-Ar_3$ and $H_2O^+-Ar_4$, respectively. Ar complexation at the oxygen atom causes partial charge transfer from Ar to the 2p orbital of oxygen and results in blue-shifting of the ν_3 frequency with respect to $H_2O^+-Ar_2$. Large incremental ν_3 shifts were observed for small complexes with n up to 4, and subsequent changes are much smaller. The ν_3 frequencies for $n = 4-14$ are all within 3000−3050 cm^{-1}, which are only slightly lower than that observed in solid argon matrix (3054.9 cm^{-1}). As the authors pointed out, the initial four Ar atoms are more strongly bound than the subsequent Ar atoms ($n = 5-14$). We suggest that the H_2O^+ cation observed in solid argon may be described as a $H_2O^+-Ar_4$ complex isolated in the argon matrix. The ν_3 mode of $H_2O^+-Ar_4$ was observed at 3008 cm^{-1} in the gas phase, which is only 46.9 cm^{-1} lower than the argon matrix value. This difference is compatible with typical Ar matrix shifts.[46] Consistent with this notion, our calculations showed that H_2O^+ could only bound as many as four argon atoms. The optimized structures of $H_2O^+-Ar_n$ ($n = 0-4$) are shown in Figure 3, and the HOH stretching vibrational frequencies are listed in Table 2. MP2 calculations predicted that the antisymmetric and symmetric HOH stretching modes of $H_2O^+-Ar_4$ red-shifted by 189.7 and 143.5 cm^{-1} with respect to those of H_2O^+, in reasonable agreement with the experimental shifts. However, the B3LYP calculations gave much smaller shifts (15.8 and 46.2 cm^{-1}).

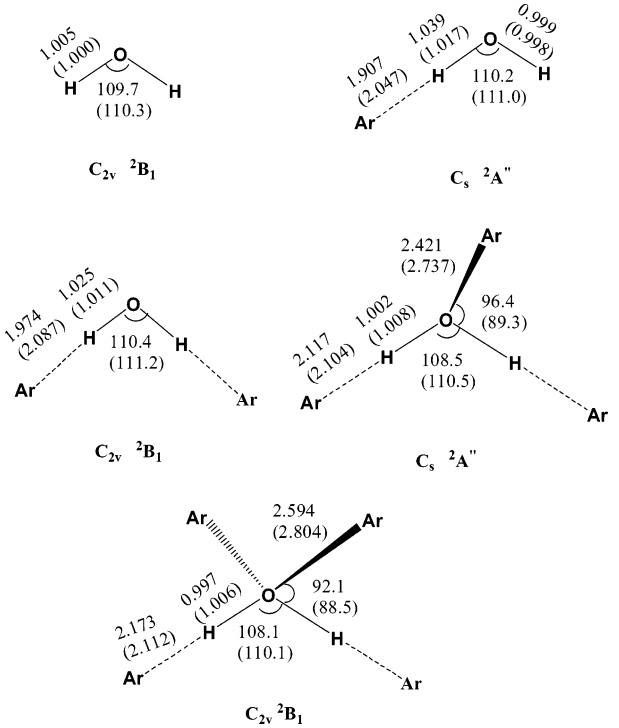

Figure 3. Optimized structures (bond lengths in Å, bond angles in degrees) of the $H_2O^+-Ar_n$ ($n = 0-4$) complexes at the B3LYP/6-311++G(3df,3pd) and MP2/6-31++g(d, p) (in parentheses) levels of theory.

TABLE 2: Calculated Stretching Vibrational Frequencies (cm^{-1}) and Intensities (km/mol) of the $H_2O^+-Ar_n$ ($n = 0-4$) Complexes at the B3LYP/6-311++G(3df, 3pd) and MP2/6-31++G(d,p) Levels of Theory

	B3LYP		MP2	
n	ν_1	ν_3	ν_1	ν_3
0	3330.2 (116)	3372.6 (453)	3442.7 (143)	3533.1 (489)
1	2672.8 (905)	3414.6(348)	3135.5 (1216)	3522.5 (376)
2	2875.0 (2165)	2920.5 (320)	3228.1 (447)	3245.0 (1909)
3	3220.9 (1096)	3270.3 (1451)	3270.9 (458)	3307.0 (1707)
4	3284.0 (471)	3356.8 (1253)	3299.2 (400)	3343.4 (1590)

OH^+. The 2979.6 cm^{-1} band is also due to a cation species on the basis of its photosensitive behavior and intensity enhancement upon CCl_4 doping. This band shifted to 2967.2 cm^{-1} with $H_2{}^{18}O$/Ar, and to 2249.1 cm^{-1} with D_2O/Ar. The $^{16}O/^{18}O$ isotopic ratio of 1.0042 is about the same as that of the HOH stretching mode of the H_2O^+ cation, whereas the H/D ratio of 1.3248 is significantly smaller than that of the H_2O^+ cation. This implies that there is less hydrogen involvement in the 2979.6 cm^{-1} mode than that in the HOH stretching mode of H_2O^+ cation. The band position and isotopic frequency ratios are suggestive of an O−H stretching vibration. In the mixed $H_2{}^{16}O + H_2{}^{18}O$ (Figure 2, trace b) and $H_2O + HDO + D_2O$ (Figure 2, trace c) spectra, only the pure isotopic counterparts were observed and clearly indicated that only one O atom and one H atom are involved in this mode. Accordingly, we assign

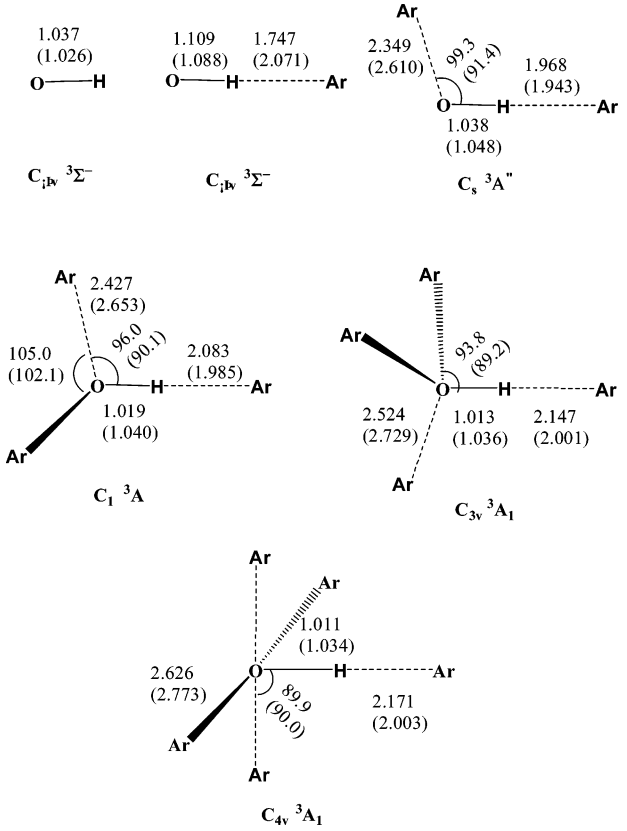

Figure 4. Optimized structures (bond lengths in Å, bond angles in degrees) of the OH^+-Ar_n ($n = 0-5$) complexes at the B3LYP/6-311++G(3df,3pd) and MP2/6-31++G(d, p) (in parentheses) levels of theory.

the 2979.6 cm^{-1} band to the O−H stretching mode of the OH^+ cation in solid argon.

The OH^+ cation has been well studied in the gas phase.[1−7] This cation has a $^3\Sigma^-$ ground state with an equilibrium bond distance of 1.0279 Å. The band center of the O−H stretching fundamental was determined to be 2956.3 cm^{-1}. Similar to the H_2O^+ cation, the OH^+ cation can form a complex with rare gas atoms. Recent investigations have shown that the open-shell OH^+ cation forms linear proton-bound complexes with He and Ne. The O−H stretching vibrational origins of the complexes red-shifted by 66.3 and 169.9 cm^{-1} with respect to the free OH^+ cation.[26] Quantum simulations indicated that the O−H stretching frequencies of the OH^+-Ne_n complexes are red-shifted with respect to OH^+. The red-shift approaches a value of about 110 cm^{-1} for large n, and hence, the frequency of OH^+ in a neon matrix is estimated to be observed at around 2845 cm^{-1}.[32] Interestingly, the OH^+ cation was observed to absorb at 2979.6 cm^{-1} in solid argon, 23.3 cm^{-1} blue-shifted from the gas-phase band center.

To have a better understanding of the vibrational shift of the OH^+ frequency as a function of the number of argon atoms surrounding the cation, quantum chemical computations were performed on the OH^+-Ar_n complexes. The calculation results showed that the $^3\Sigma^-$ ground-state OH^+ cation could bound as many as five argon atoms with one argon attached to the H atom and four argon atoms attached to the opposite sites of the $2p_x$ and $2p_y$ orbitals of oxygen. The optimized geometric parameters for OH^+-Ar_n with $n = 0-5$ are shown in Figure 4, and the O−H stretching vibrational frequencies are listed in Table 3. On the basis of the calculations, Ar complexation at the hydrogen atom elongates the O−H bond length and results in red-shifting of the O−H stretching frequency, whereas argon binding to the oxygen atom decreases the O−H bond length and results in blue-shifting of the O−H stretching frequency. According to the MP2 calculations, the global minimum of OH^+-Ar_n has a linear or near-linear proton-bound structure for $n = 1-5$ (Figure 4). As shown in Table 3, the argon complexation induced a red-shift of the O−H stretching frequency. The red-shift decreases as the number of argon atoms increases. In contrast to the MP2 calculations, B3LYP calculations predicted that the O−H stretching frequency of OH^+-Ar_n first red-shifted but blue-shifted once $n \geq 3$. As has been pointed out previously,[33,49,50] DFT and MP2 calculations are expected to provide poor vibrational frequency predictions on the weakly bound rare gas complexes. Apparently, higher level calculations will have to be performed to fit the experimental value.

TABLE 3: Calculated OH Stretching Vibrational Frequencies (cm^{-1}) of the OH^+-Ar_n ($n = 0-5$) Complexes at the B3LYP/6-311++G(3df,3pd) and MP2/6-31++G(d, p) Levels of Theory

	frequency	
n	B3LYP	MP2
0	3041.7	3238.0
1	1912.8	2507.0
2	2776.0	2743.6
3	3054.4	2864.3
4	3138.8	2926.9
5	3169.4	2946.6

Conclusions

The OH^+ and H_2O^+ cations have been produced by co-deposition of H_2O/Ar mixture with high-frequency-discharged Ar at 4 K. Infrared absorption spectra of various OH^+ and H_2O^+ isotopomers solvated in solid argon were recorded. On the basis of isotopic substitution studies, absorptions at 3054.9 and 3040.0 cm^{-1} are assigned to the antisymmetric and symmetric H−O−H stretching vibrations of H_2O^+, and absorption at 2979.6 cm^{-1} is assigned to the O−H stretching vibration of OH^+. The frequencies of H_2O^+ solvated in solid argon are red-shifted, whereas the frequency of OH^+ is blue-shifted with respect to the gas-phase fundamentals. Both the OH^+ and H_2O^+ cations can form complexes with argon atoms, and the cations solvated in solid argon may be regarded as the OH^+-Ar_5 and $H_2O^+-Ar_4$ complexes isolated in the argon matrix on the basis of previous gas-phase studies as well as of quantum chemical calculations.

Acknowledgment. We greatly acknowledge financial support from the NNSFC (Grant No. 20433080 and 20473023) and the Committee of Science and Technology of Shanghai (04JC14016).

References and Notes

(1) Merer, A. J.; Malm, D. N.; Martin, R. W.; Horani, M.; Rostas, J. *Can. J. Phys.* **1975**, *53*, 251.

(2) Crofton, M. W.; Altman, R. S.; Jagod, M. F.; Oka, T. *J. Phys. Chem.* **1985**, *89*, 3614. Liu, D. J.; Ho, W. C.; Oka, T. *J. Chem. Phys.* **1987**, *87*, 2442. Rehfuss, B. D.; Jagod, M. F.; Xu, L. W.; Oka, T. *J. Mol. Spectrosc.* **1992**, *151*, 59.

(3) Verhoeve, P.; Bekooy, J. P.; Meerts, W. L.; Ter Meuwlen, J. J.; Dynamus, A. *Chem. Phys. Lett.* **1986**, *125*, 286.

(4) Gruebele, M. H. W.; Muller, R. P.; Saykally, R. J. *J. Chem. Phys.* **1986**, *84*, 2489. Gruebele, M. H. W.; Keim, E.; Stein, A.; Saykally, R. J. *J. Mol. Spectrosc.* **1988**, *131*, 343.

(5) Rodgers, D. J.; Sarre, P. J. *Chem. Phys. Lett.* **1988**, *143*, 235.

(6) Bae, Y. K. *Chem. Phys. Lett.* **1991**, *180*, 179.

(7) Varberg, T. D.; Evenson, K. M.; Brown, J. M. *J. Chem. Phys.* **1994**, *100*, 2487.

(8) Brundle, C. R.; Turner, D. W. *Proc. R. Soc. London* **1968**, *A 307*, 27.
(9) Lew, H. *Can. J. Phys.* **1976**, *54*, 2028.
(10) Reutt, J. E.; Wang, L. S.; Lee, Y. T.; Shirley, D. A. *J. Chem. Phys.* **1986**, *85*, 6928.
(11) Strahan, S. E.; Mueller, R. P.; Saykally, R. J. *J. Chem. Phys.* **1986**, *85*, 1252.
(12) Dinelli, B. M.; Crofton, M. W.; Oka, T. *J. Mol. Spectrosc.* **1988**, *127*, 1. Huet, T. R.; Pursell, C. J.; Ho, W. C.; Dinelli, B. M.; Oka, T. *J. Chem. Phys.* **1992**, *97*, 5977.
(13) Brown, P. R.; Davies, P. B.; Stickland, R. J. *J. Chem. Phys.* **1989**, *91*, 384.
(14) Das, B.; Farley, J. W. *J. Chem. Phys.* **1991**, *95*, 8809.
(15) Tonkyn, R. G.; Wiedmann, R.; Grant, E. R.; White, M. G. *J. Chem. Phys.* **1991**, *95*, 7033.
(16) Merkt, F.; Signorell, R.; Palm, H.; Osterwalder, A.; Sommavilla, M. *Mol. Phys.* **1998**, *95*, 1045.
(17) Rosmus, P.; Meyer, W. *J. Chem. Phys.* **1977**, *66*, 13. Werner, H. J.; Rosmus, P.; Reinsch, E. A. *J. Chem. Phys.* **1983**, *79*, 905.
(18) Hirst, D. M.; Guest, M. F. *Mol. Phys.* **1983**, *49*, 1461.
(19) Saxon, R. P.; Liu, B. *J. Chem. Phys.* **1986**, *85*, 2099.
(20) Adamowicz, L. *J. Chem. Phys.* **1988**, *89*, 6305.
(21) Yarkony, D. R. *J. Phys. Chem.* **1992**, *97*, 111.
(22) Jackels, C. F. *J. Chem. Phys.* **1980**, *72*, 4873.
(23) Degli Esposti, A.; Lister, D. G.; Palmieri, P.; Degli Esposti, C. *J. Chem. Phys.* **1987**, *87*, 6772.
(24) Weis, B.; Carter, S.; Rosmus, P.; Werner, H. J.; Knowles, P. J. *J. Chem. Phys.* **1989**, *91*, 2818. Brommer, M.; Weis, B.; Follmeg, B.; Rosmus, P.; Carter, S.; Handy, N. C.; Werner, H. J.; Knowles, P. J. *J. Chem. Phys.* **1993**, *98*, 5222. Weis, B.; Yamashita, K. *J. Chem. Phys.* **1993**, *99*, 9512.
(25) Lopez, G. E. *J. Comput. Chem.* **1995**, *16*, 768.
(26) Roth, D.; Nizkorodov, S. A.; Maier, J. P.; Dopfer, O. *J. Chem. Phys.* **1998**, *109*, 3841.
(27) Dopfer, O.; Roth, D.; Maier, J. P. *J. Chem. Phys.* **2001**, *114*, 7081.
(28) Dopfer, O.; Roth, D.; Maier, J. P. *J. Phys. Chem. A* **2000**, *104*, 11702.
(29) Dopfer, O.; Eugel, V. *J. Chem. Phys.* **2004**, *121*, 12345.
(30) Hughes, J. M.; Nagy-Felsobuki, E. I. *J. Phys. Chem. A* **1997**, *101*, 3995.
(31) Meuwly, M.; Maier, J. P.; Rosmus, P. *J. Chem. Phys.* **1998**, *109*, 3850.
(32) Meuwly, M. *J. Phys. Chem. A* **2000**, *104*, 7144.
(33) Dopfer, O. *J. Phys. Chem. A* **2000**, *104*, 11693.
(34) Forney, D.; Jacox, M. E.; Thompson, W. E. *J. Chem. Phys.* **1993**, *98*, 841.
(35) Chen, M. H.; Wang, X. F.; Zhang, L. N.; Yu, M.; Qin, Q. Z. *Chem. Phys.* **1999**, *242*, 81.
(36) Kong, Q. Y.; Zeng, A. H.; Chen, M. H.; Zhou, M. F.; Xu, Q. *J. Chem. Phys.* **2003**, *118*, 7267. Kong, Q. Y.; Zeng, A. H.; Chen, M. H.; Xu, Q.; Zhou, M. F. *J. Phys. Chem. A* **2004**, *108*, 1531.
(37) Frisch, M. J.; Trucks, G. W.; Schlegel, H. B.; Scuseria, G. E.; Robb, M. A.; Cheeseman, J. R.; Montgomery, J. A., Jr.; Vreven, T.; Kudin, K. N.; Burant, J. C.; Millam, J. M.; Iyengar, S. S.; Tomasi, J.; Barone, V.; Mennucci, B.; Cossi, M.; Scalmani, G.; Rega, N.; Petersson, G. A.; Nakatsuji, H.; Hada, M.; Ehara, M.; Toyota, K.; Fukuda, R.; Hasegawa, J.; Ishida, M.; Nakajima, T.; Honda, Y.; Kitao, O.; Nakai, H.; Klene, M.; Li, X.; Knox, J. E.; Hratchian, H. P.; Cross, J. B.; Adamo, C.; Jaramillo, J.; Gomperts, R.; Stratmann, R. E.; Yazyev, O.; Austin, A. J.; Cammi, R.; Pomelli, C.; Ochterski, J. W.; Ayala, P. Y.; Morokuma, K.; Voth, G. A.; Salvador, P.; Dannenberg, J. J.; Zakrzewski, V. G.; Dapprich, S.; Daniels, A. D.; Strain, M. C.; Farkas, O.; Malick, D. K.; Rabuck, A. D.; Raghavachari, K.; Foresman, J. B.; Ortiz, J. V.; Cui, Q.; Baboul, A. G.; Clifford, S.; Cioslowski, J.; Stefanov, B. B.; Liu, G.; Liashenko, A.; Piskorz, P.; Komaromi, I.; Martin, R. L.; Fox, D. J.; Keith, T.; Al-Laham, M. A.; Peng, C. Y.; Nanayakkara, A.; Challacombe, M.; Gill, P. M. W.; Johnson, B.; Chen, W.; Wong, M. W.; Gonzalez, C.; Pople, J. A. *Gaussian 03*, Revision B.05; Gaussian, Inc.: Pittsburgh, PA, 2003.
(38) Becke, A. D. *J. Chem. Phys.* **1993**, *98*, 5648. Lee, C.; Yang, E.; Parr, R. G. *Phys. Rev. B* **1988**, *37*, 785.
(39) Moller, C.; Plesset, M. S. *Phys. Rev. B* **1984**, *46*, 618.
(40) McLean, A. D.; Chandler, G. S. *J. Chem. Phys.* **1980**, *72*, 5639. Krishnan, R.; Binkley, J. S.; Seeger, R.; Pople, J. A. *J. Chem. Phys.* **1980**, *72*, 650.
(41) Cheng, B. M.; Lee, Y. P.; Ogilvie, J. F. *Chem. Phys. Lett.* **1988**, *151*, 109.
(42) Langford, V. S.; McKinley, A. J.; Quickenden, T. I. *J. Am. Chem. Soc.* **2000**, *122*, 12859. Cooper, P. D.; Kjaergaard, H. J.; Langford, V. S.; McKinley, A. J.; Quichenden, T. I.; Schofield, D. P. *J. Am. Chem. Soc.* **2003**, *125*, 6048.
(43) Milligan, D. E.; Jacox, M. E. *J. Chem. Phys.* **1963**, *38*, 2627. Smith, D. W.; Andrews, L. *J. Chem. Phys.* **1974**, *60*, 81.
(44) Zhou, M. F.; Andrews, L. *J. Am. Chem. Soc.* **1998**, *120*, 11499. Zhou, M. F.; Andrews, L. *J. Am. Chem. Soc.* **1998**, *120*, 13230.
(45) Zhou, M. F.; Zeng, A. H.; Wang, Y.; Kong, Q. Y.; Wang, Z. X.; Schleyer, P. V. R. *J. Am. Chem. Soc.* **2003**, *125*, 11512.
(46) Jacox, M. E. *Chem. Phys.* **1994**, *189*, 149.
(47) Shinohara, H.; Nishi, N.; Washida, N. *J. Chem. Phys.* **1986**, *84*, 5561. Shiromaru, H.; Shinohara, H.; Washida, N.; Yoo, H. S.; Kimura, K. *Chem. Phys. Lett.* **1987**, *141*, 7.
(48) Vaidyanathan, G.; Coolbaugh, M. T.; Peifer, W. R.; Garvey, J. F. *J. Phys. Chem.* **1991**, *95*, 4193.
(49) Fridgen, T. D.; Parnis, J. M. *J. Chem. Phys.* **1998**, *109*, 2162.
(50) Beyer, M.; Savchenko, E. V.; Niedner-Schatteburg, G.; Bondybey, V. E. *J. Chem. Phys.* **1999**, *110*, 11950.